Catal Lett (2012) 142:714–717
DOI 10.1007/s10562-012-0815-3

Dehydrogenation of Propane to Propylene over Supported Model Ni–Au Catalysts

Zhen Yan · Yunxi Yao · D. Wayne Goodman

Received: 24 January 2012 / Accepted: 20 March 2012 / Published online: 10 April 2012

Abstract Hydrogenolysis and dehydrogenation of propane were studied over model nickel–gold catalysts. The supported model Ni–Au catalysts were prepared by depositing Ni and Au onto a planar silica film. Infrared reflection absorption spectroscopic data showed that isolated Ni sites appeared and became dominant on the surface with the addition of Au to Ni. For the conversion of propane in the presence of hydrogen, the dehydrogenation of propane to propylene was observed on the Ni–Au bimetallic catalysts, whereas only hydrogenolysis products were observed on the monometallic Ni catalyst. A correlation was found between the concentration of isolated Ni sites and the catalytic activity for propane dehydrogenation.

Keywords Bimetallic catalysts · Model catalysts · Nickel · Gold · Dehydrogenation · Propane · Propylene

1 Introduction

Nickel–gold bimetallic catalysts have been shown to have promising catalytic properties for a variety of reactions [1–9], such as steaming reforming of hydrocarbons [1, 2], the water–gas shift reaction [3], hydrodechlorination [4, 5] and selective hydrogenation of alkynes [6]. Besenbacher et al. showed that the activity of a $MgAl_2O_4$-supported Ni–Au catalyst was almost constant for the steam reforming of *n*-butane, whereas a pure Ni catalyst deactivated rapidly [1]. Venugopal et al. found that a bimetallic Au–Ni/Fe_2O_3 catalyst was more active than Au/Fe_2O_3 for the water–gas shift reaction [3]. Yuan et al. reported that the addition of Au to silica-supported Ni catalysts significantly enhanced the activity of 2,4-dichlorophenol hydrodechlorination [4, 5]. So far, the beneficial effects of the Ni–Au bimetallic system have been limited to higher catalytic activities or better catalyst stabilities; the selectivity effects have not been explored to a great extent.

Recently we have prepared model Ni–Au catalysts supported on planar silica films and propane hydrogenolysis was then used as a probe reaction to study the properties of these bimetallic catalysts. It is well known that the reaction of propane on supported Ni catalysts in the presence of hydrogen forms only hydrogenolysis products (methane and ethane) [10–12] and the dehydrogenation product, i.e. propylene has not been observed due to the strong ability of nickel to catalyze C–C bond cleavage [13]. In the present work, we report that by modifying the surface composition and structure of Ni catalysts with Au, the reaction of propane in the presence of hydrogen can be shifted from hydrogenolysis to dehydrogenation.

2 Experimental

The experiments were carried out in two ultrahigh vacuum chambers. One was equipped with X-ray photoelectron spectroscopy and a high-pressure reaction cell, and the other was equipped with Auger electron spectroscopy, polarization modulation infrared reflection absorption spectroscopy (PM–IRAS), and TPD [14, 15]. The Ni–Au catalysts were synthesized on a planar SiO_2 film ($\sim$10 nm thick) prepared by evaporating Si on a molybdenum single crystal (10 mm in diameter) in a background of 1.0×10^{-5}

Dr. Goodman deceased on February 27, 2012.

Z. Yan · Y. Yao · D. W. Goodman (✉)
Department of Chemistry, Texas A and M University, College Station, TX 77843, USA
e-mail: goodman@mail.chem.tamu.edu

Torr oxygen at room temperature, followed by oxidation at 1,200 K [16, 17]. The monometallic Ni/SiO_2 catalyst was prepared by vapor-depositing five monolayers equivalent (MLE) of Ni on the SiO_2 film, followed by annealing to 700 K. The average particle size of Ni estimated from CO TPD experiments was 5 ± 1 nm, which is in good agreement with previous studies [18]. Bimetallic Ni–Au/SiO_2 catalysts were prepared by depositing various amounts of Au on 5 MLE Ni/SiO_2 and annealing to 700 K.

Catalytic reactions were carried out in a batch reactor (0.2 L) using 1:5:45 $C_3H_8/H_2/N_2$ mixtures at a total pressure of 20 Torr. After 5 min of reaction, the gas mixture was withdrawn and the products were analyzed with a HP 5890 gas chromatograph equipped with a flame ionization detector and a HP-PLOT Al_2O_3 capillary column. The selectivity is defined as the moles of carbon in each product normalized by the total moles of carbon of the products, so that the total selectivity of all carbon containing products equals 100 %. Blank experiments carried out on SiO_2 film and Au/SiO_2 showed that there was no background activity under our reaction conditions.

3 Results and Discussion

Figure 1a shows the room temperature PM-IRAS spectra after saturation exposure of carbon monoxide on Ni–Au/SiO_2 surfaces with increasing Au coverages. The IRAS spectrum of the monometallic Ni/SiO_2 catalyst shows two stretching features at 2,055 and 1,950 cm^{-1}, corresponding to CO adsorbed on atop Ni sites (linearly bound CO) and on two-fold bridging Ni sites, respectively [19, 20]. The broad IRAS features are due to CO adsorption on different crystal faces (e.g. Ni(111) and Ni(100)) and on different sized Ni nanoparticles [18]. With the addition of Au, the intensity of the atop CO peak increased significantly and reached a maximum before starting to decline. On the other hand, the bridge-bound CO peak decreased quickly with the addition of Au and completely disappeared on the 1 MLE Au-5 MLE Ni surface. The absence of CO adsorption on bridging Ni sites indicates that there are no neighboring Ni atoms on the surface and all the surface Ni atoms are isolated by Au atoms. The area of the atop CO peak as a function of Au coverage is shown in Fig. 1b. The highest intensity was observed on the 1.5 MLE Au-5 MLE Ni surface. Beyond that, the atop CO peak began to decrease because the number of surface Ni atoms decreased with further Au deposition. It is noteworthy that the CO stretching frequencies are higher at low Au coverages as seen in Fig. 1a, which is caused by dipole–dipole coupling among CO molecules [21].

Figure 2 shows the reaction rate of propane at 523 K as a function of Au coverage on Au-5 MLE Ni/SiO_2 catalysts. The decrease in the reaction rate is consistent with the IRAS results that Au and Ni form surface alloy and active surface Ni atoms are replaced by inactive Au atoms. The formation rate of propylene and its selectivity are shown in Fig. 3. On the monometallic Ni/SiO_2 catalyst, methane was the dominant product and no propylene was detected. With the addition of 0.5 MLE Au, a small amount of propylene was formed with a selectivity of ~1 %. As more Au was deposited on the Ni/SiO_2 surface, the formation rate of propylene kept increasing and reached a maximum at a Au coverage of 1.5 MLE, at which point the selectivity to propylene was 20 %. The propylene selectivity continued to increase at Au coverages higher than 1.5 MLE, whereas the formation rate of propylene began to decline as a result of lower propane conversions. In the meantime, the

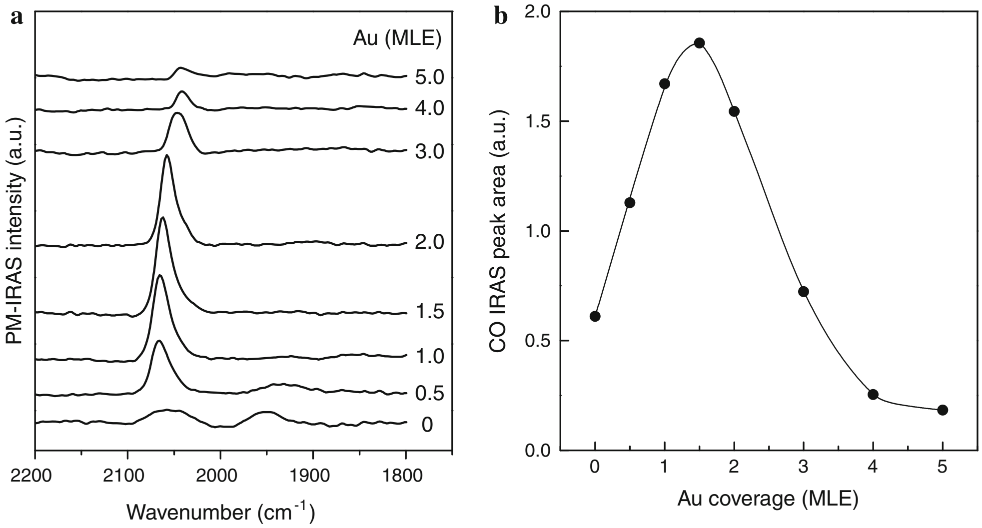

Fig. 1 **a** Room temperature PM–IRAS spectra of saturated CO adsorption on Au-5 MLE Ni/SiO_2 surfaces with varying Au coverage as indicated. **b** IRAS peak area of the atop adsorbed CO as a function of Au coverage

distribution of hydrogenolysis products, i.e. methane vs. ethane and ethylene, also changed significantly with the addition of Au. The selectivity to C_2 products (not shown in the figure) increased from ~1 % on the monometallic Ni catalyst to 15 % on the 1.5 MLE Au–Ni catalyst.

The direct correlation between the concentration of atop Ni sites (Fig. 1b) and the formation rate of propylene (Fig. 3) suggests that propane dehydrogenation occurs on isolated Ni atoms. It has been well-established that the hydrogenolysis of light alkanes is a structure sensitive reaction and requires multiple adjacent surface atoms or ensembles to proceed [22–25]. Martin et al. showed that ensembles of between 12 and 20 adjacent nickel atoms were required for the hydrogenolysis of C_2–C_4 alkanes [26]. On the other hand, the dehydrogenation of propane on supported Pt catalysts has been found to be structure-insensitive and it was proposed that only one Pt atom was involved in the rate-determining step [27]. According to the proposed pathways of hydrogenolysis, propane adsorbs on the surface dissociatively and then undergoes further dehydrogenation. The dehydrogenated C_3H_x species adsorbs on Ni ensembles with a favorable geometry, resulting in the weakening and breaking of C–C bonds. With the addition of Au, the number of suitable ensembles decreases sharply and isolated Ni sites start to appear on the surface. For C_3H_x species adsorbed on single Ni atoms, it is reasonable to assume that the C–C bond breaking became energetically unfavorable, and as a result, the dehydrogenation product is formed. The correlation found between Figs. 1b and 3 is consistent with the dehydrogenation of propane being catalyzed by single Ni atoms.

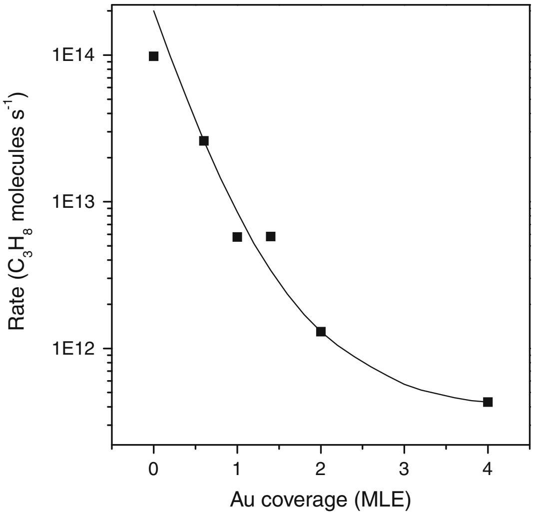

Fig. 2 Reaction rate of propane at 523 K as a function of Au coverage on Au-5MLE Ni/SiO_2 catalysts

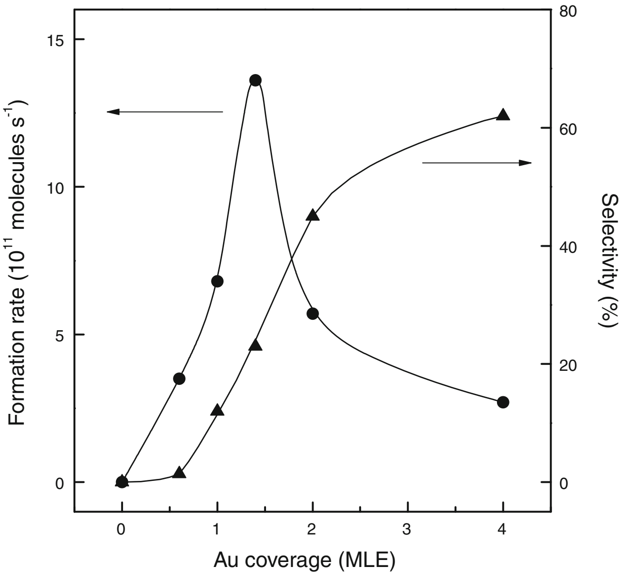

Fig. 3 Propylene formation rate and selectivity as a function of Au coverage

Similar effects arising from the addition of inactive metals to ensembles of active metals have been observed in other catalytic systems. In his classic work on bimetallic catalysts [24], Sinfelt showed that the activity of Ni for ethane hydrogenolysis decreased by five orders of magnitude with the addition of Cu, whereas the activity for cyclohexane dehydrogenation was not affected over a wide range of composition. In a recent study, Chen et al. reported that Pd monomers isolated by Au were much more active than contiguous Pd atoms for the synthesis of vinyl acetate and the formation of isolated Pd atoms was believed to inhibit the formation of undesirable by-products [28]. Similarly, high yields were observed on carbon-supported Pd–Au catalysts for the direct synthesis of hydrogen peroxide, presumably due to decoration and inhibition of the sites for the decomposition reaction [29].

The conversion of propane was also studied in a plug-flow reactor system using real supported Ni–Au catalysts prepared by the conventional impregnation method from high–surface-area silica [30]. Under similar partial pressures of propane and hydrogen, the formation of propylene was observed on the Ni–Au/SiO_2 catalysts, but not on monometallic Ni/SiO_2, confirming our findings on the model catalysts.

4 Conclusions

The IRAS data presented in this paper support that isolated Ni sites are formed on the surface of the model Ni–Au catalysts. For the conversion of propane in the presence of H_2, the dehydrogenation of propane to propylene was observed on the bimetallic Ni–Au catalysts, whereas only hydrogenolysis products were observed on the monometallic Ni catalyst. A direct correlation was found between the concentration of isolated Ni sites and the catalytic activity for propane dehydrogenation.

Acknowledgments We gratefully acknowledge the support for this work by the US Department of Energy, Office of Basic Energy Sciences, Division of Chemical Sciences, Geosciences, and Bio-sciences (DE-FG02-95ER-14511), and the Robert A. Welch Foundation (A-300).

References

1. Besenbacher F, Chorkendorff I, Clausen BS, Hammer B, Molenbroek AM, Nørskov JK, Stensgaard I (1998) Science 279:1913
2. Chin Y-H, King DL, Roh H-S, Wang Y, Heald SM (2006) J Catal 244:153
3. Venugopal A, Aluha J, Scurrell MS (2003) Catal Lett 90:1
4. Keane MA, Gómez-Quero S, Cárdenas-Lizana F, Shen W (2009) ChemCatChem 1:270
5. Yuan G, Lopez JL, Louis C, Delannoy L, Keane MA (2005) Catal Commun 6:555
6. Nikolaev SA, Smirnov VV, Vasil'kov AY, Podshibikhin VL (2010) Kinet Catal 51:375
7. Suo Z, Lv A, Lv H, Jin M, He T (2009) Catal Commun 10:1174
8. Chandler BD, Long CG, Gilbertson JD, Pursell CJ, Vijayaraghavan G, Stevenson KJ (2010) J Phys Chem C 114:11498
9. Jiang H-L, Umegaki T, Akita T, Zhang X-B, Haruta M, Xu Q (2010) Chem Eur J 16:3132
10. Machiels CJ, Anderson RB (1979) J Catal 58:253
11. Guilleux MF, Dalmon JA, Martin GA (1980) J Catal 62:235
12. Shephard FE (1969) J Catal 14:148
13. Sinfelt JH (1970) Catal Rev Sci Eng 3:175
14. Yan Z, Wang Z, Bukur DB, Goodman DW (2009) J Catal 268:196
15. Ozensoy E, Meier DC, Goodman DW (2002) J Phys Chem B 106:9367
16. Xu X, Goodman DW (1992) Appl Phys Lett 61:774
17. Xu X, Goodman DW (1993) Surf Sci 282:323
18. Coulter K, Xu X, Goodman DW (1994) J Phys Chem 98:1245
19. Campuzano JC, Greenler RG (1979) Surf Sci 83:301
20. Trenary M, Uram KJ, Yates JT Jr (1985) Surf Sci 157:512
21. Hoffmann FM (1983) Surf Sci Rep 3:107
22. Goodman DW (1982) Surf Sci Lett 123:L679
23. Martin GA (1988) Catal Rev Sci Eng 30:519
24. Sinfelt JH, Carter JL, Yates DJC (1972) J Catal 24:283
25. Sachtler WMH (1982) Faraday Discuss Chem Soc 72:7
26. Dalmon JA, Martin GA (1980) J Catal 66:214
27. Biloen P, Dautzenberg FM, Sachtler WMH (1977) J Catal 50:77
28. Chen M, Kumar D, Yi C-W, Goodman DW (2005) Science 310:291
29. Edwards JK, Solsona B, Ntainjua EN, Carley AF, Herzing AA, Kiely CJ, Hutchings GJ (2009) Science 323:1037
30. Yan Z, Goodman DW (2012) Catal Lett. doi:10.1007/s10562-012-0791-7